別紙8 「予後」データシート

別紙8 「予後」データシート　　Ver. 316

グラスゴー・コーマ・スケール

	開眼	発語	運動機能
蘇生2週間後			
	4 自発的に	5 指南力良好	6 命令に従う
	3 呼びかけにより	4 会話混乱	5 局部的に動く
	2 疼痛により	3 不適当な発語	4 逃避反応
	1 開眼せず	2 理解不明の声	3 異常な屈曲反応
		1 発語せず	2 進展反応
			1 全く動かず

グラスゴー・ピッツバーグ脳機能カテゴリー

蘇生1ヶ月後	
蘇生6ヶ月後	

1 機能良好

意識清明。日常の生活と労働が可能。障害があっても軽度の構音障害、脳神経障害、不全麻痺など軽い神経障害あるいは精神障害まで。

2 中等度障害

意識あり。限られた環境でのパートタイム労働や日常生活(着衣行動、公共の乗り物を使っての移動、食事の準備)は自立してできる。片麻痺、嚥下障害、痙攣、構語障害、記憶障害、精神障害は残ってもよい。

3 高度障害

意識はあるが、認識制限がある。日常生活を営むのに他者の解除を要する。大脳障害として、歩行はできるものの高度の記憶障害や痴呆のあるものから、locked-inのように目で合図することしかできないものまで幅が広い。

4 昏睡、植物状態

意識なし、認識の欠如。言語反応や精神的交流の欠如。

5 死亡

脳死もしくは死亡

	年	月	日	時	分
ICU生存退室日					
生存退院日					
死亡した日付					

別紙9　Barthel index (Mahoney FI, Md St Med J 1965, 14, 61-65)

食事
- 10. 自立，自助具などの装着可，標準的時間内に食べ終える
- 5. 部分介助(たとえば，おかずを切って細かくしてもらう)
- 0. 全介助

移動
- 15. 自立，ブレーキ，フットレストの操作も含む(非行自立も含む)
- 10. 軽度の部分介助または監視を要する
- 5. 座ることは可能であるがほぼ全介助
- 0. 全介助または不可能

整容
- 5. 自立(洗面，整髪，歯 磨き，ひげ剃り)
- 0. 部分介助または不可能

トイレ動作
- 10. 自立(衣服の操作，後始末を含む，ポータブル便器などを使用している場合はその洗浄も含む)
- 5. 部分介助，体を支える，衣服，後始末に介助を要する
- 0. 全介助または不可能

入浴
- 5. 自立
- 0. 部分介助または不可能

歩行
- 15. 45M 以上の歩行，補装具(車椅子，歩行器は除く)の使用の有無は問わず
- 10. 45M 以上の介助歩行，歩行器の使用を含む
- 5. 歩行不能の場合，車椅子にて 45M 以上の操作可能
- 0. 上記以外

階段昇降
- 10. 自立，手すりなどの使用の有無は問わない
- 5. 介助または監視を要する
- 0. 不能

着替え
- 10. 自立，靴，ファスナー，装具の着脱を含む
- 5. 部分介助，標準的な時間内，半分以上は自分で行える
- 0. 上記以外

排便コントロール
- 10. 失禁なし，浣腸，坐薬の取り扱いも可能
- 5. ときに失禁あり，浣腸，坐薬の取り扱いに介助を要する者も含む
- 0. 上記以外

排尿コントロール
- 10. 失禁なし，収尿器の取り扱いも可能
- 5. ときに失禁あり，収尿器の取り扱いに介助を要する者も含む
- 0. 上記以外

別紙10　グラスゴー・コーマ・スケール

開眼

自発的に	4
呼びかけにより	3
疼痛により	2
開眼せず	1

発語

指南力良好	5
会話混乱	4
不適当な発語	3
理解不明の声	2
発語せず	1

運動機能

命令に従う	6
局部的に動く	5
逃避反応	4
異常な屈曲反応	3
進展反応	2
全く動かず	1

別紙11　グラスゴー・ピッツバーグ脳機能カテゴリー

1 機能良好

意識清明．日常の生活と労働が可能．障害があっても軽度の構音障害，脳神経障害，不全麻痺など軽い神経障害あるいは精神障害まで．

2 中等度障害

意識あり．限られた環境でのパートタイム労働や日常生活（着衣行動，公共の乗り物を使っての移動，食事の準備）は自立してできる．片麻痺，嚥下障害，痙攣，構語障害，記憶障害，精神障害は残ってもよい．

3 高度障害

意識はあるが，認識制限がある．日常生活を営むのに他者の解除を要する．大脳障害として，歩行はできるものの高度の記憶障害や痴呆のあるものから，locked-in のように目で合図することしかできないものまで幅が広い．

4 昏睡，植物状態

意識なし，認識の欠如．言語反応や精神的交流の欠如．

5 死亡

脳死もしくは死亡

別紙12　SIRS 診断基準, ALI 診断基準

SIRS 診断基準

以下のうち 2 項目以上が該当するとき

体温 38℃以上もしくは 36℃以下

心拍数 90 回／分以上

呼吸数 20 回／分以上もしくは PaCO2＜32mmHg

WBC12000／mm3 以上もしくは 4000／mm3 以下もしくは未熟顆粒球 10%以上

ALI 診断基準

発症様式 急性発症

酸素化能 PaO2/FiO2≦300mmHg(PEEP レベルを問わない)

胸部X線像で両側性浸潤影

肺動脈楔入圧 18mmHg 以下もしくは臨床的に左房圧上昇の所見がない

臨床研究ＷＥＢサイト

【トップページ】

【和文ページ、咽頭冷却の説明】

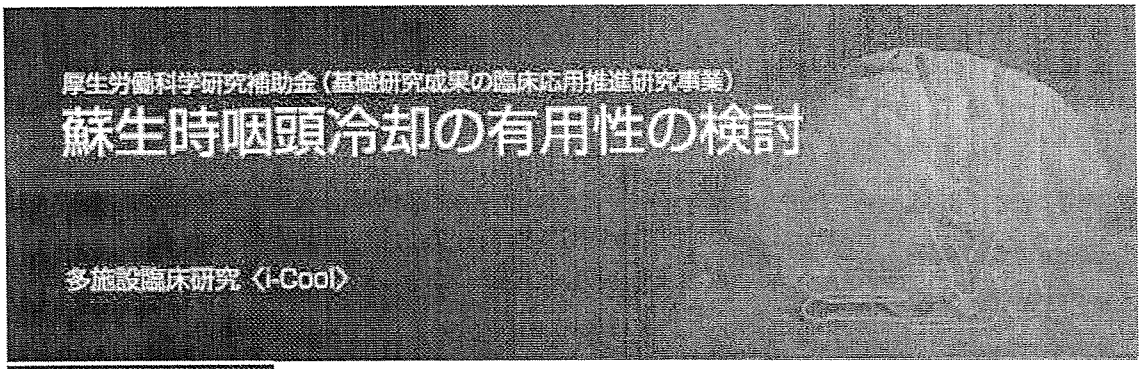

トップページ
参加施設
咽頭冷却とは
咽頭冷却カフ
冷却水還流装置
プロトコル
データシート

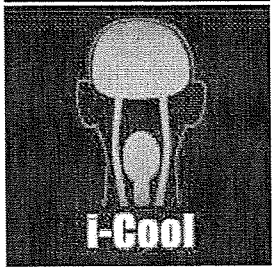

咽頭冷却とは

蘇生後意識障害の治療法として脳低温療法の有効性が報告されています。 しかし、現在の脳低温療法は全身冷却を行っているため脳温の低下に時間がかかります。 もし、頭部のみ冷却することができれば早期に脳温を低下できると考えられます。 咽頭の1cm外側を総頸動脈が走行しています。 咽頭を冷却すると、総頸動脈が冷却され血行性に脳温が低下します。 この研究では、心停止蘇生時に咽頭冷却を施行し、脳温低下効果を検証します。 また、神経学的予後、生命予後を改善する効果があるか観察します。

気管挿管で気道確保した後、咽頭冷却カフを挿入します。 咽頭冷却カフは咽頭の形状にフィットするように作られています。 5℃の生理的食塩水が500mL/分で灌流します。

【和文ページ、咽頭冷却カフの説明】

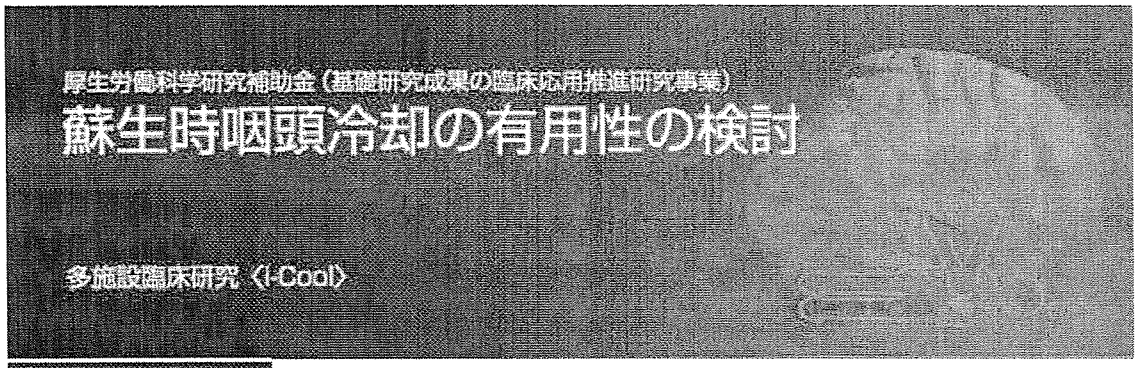

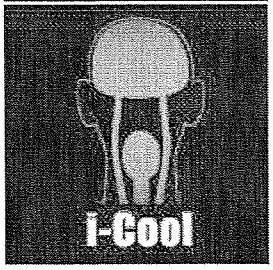

咽頭冷却カフ

カフは塩化ビニル製で生物学的安全性試験を通過しています。 咽頭の3D-CTモデルを元に作成しており、食道閉鎖式エアウェイと同様の手技で簡単に咽頭内に挿入することができます。 頸動脈は咽頭の後側方を走行するため、後側方粘膜に対する密着性が高められています。 カフ（風船部分、耐圧限界200cmH2O）内を冷却液が500mL/分、50cmH2Oの圧力で灌流します。

咽頭冷却カフの作成

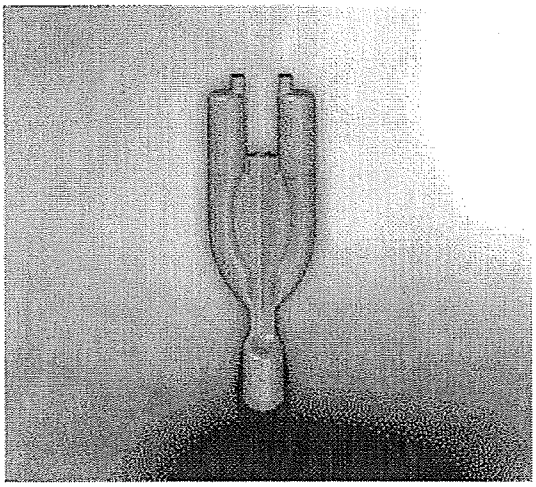

カフをCAD上で作成

【和文ページ、潅流装置の説明】

厚生労働科学研究補助金（基礎研究成果の臨床応用推進研究事業）

蘇生時咽頭冷却の有用性の検討

多施設臨床研究〈i-Cool〉

トップページ
参加施設
咽頭冷却とは
咽頭冷却カフ
冷却水還流装置
プロトコル
データシート

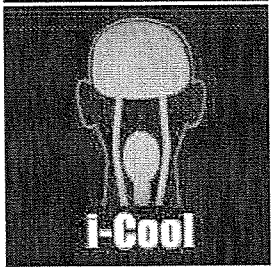

冷却水還流装置

生理食塩水を急速に冷却し、500mL/分の速度で咽頭冷却カフ内を潅流させる能力を持つ。咽頭冷却カフ内臓のセンサーより内圧・温度情報を4msec毎に収集しリアルタイムにコントロールする。

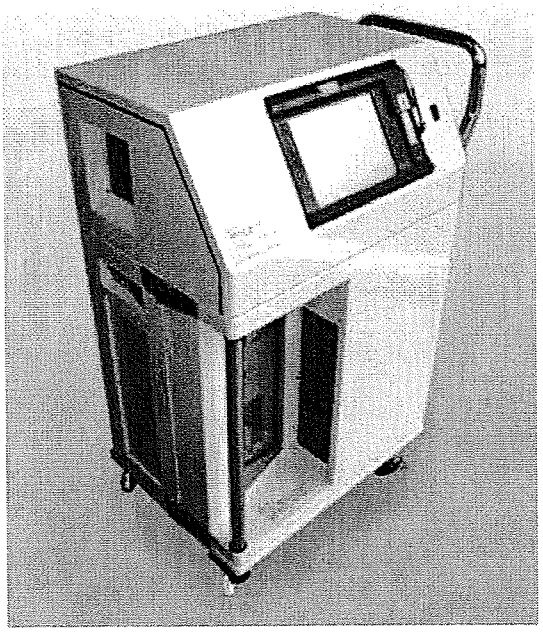

鼓膜温記録装置

コントロール群や咽頭冷却後の鼓膜温記録に使用する鼓膜温記録装置。

【英文ページ、咽頭冷却の説明】

Health and Labour Sciences Research Grant (Translational Research)

Investigation of Clinical Utility of Pharyngeal Cooling During Resuscitation

Multicenter Clinical Study 〈I-Cool〉

Top Page
Organization
What is Pharyngeal Cooling?
Pharyngeal Cooling Cuff
Circulator
Protocol
日本語ページ

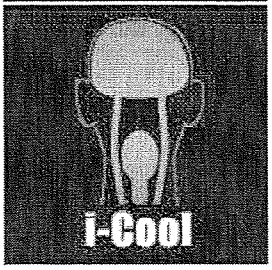

What is Pharyngeal Cooling?

Brain hypothermia has been reported as an effective therapy for post-resuscitative disturbance of consciousness. However, because current brain hypothermia involves systemic cooling, time is required to lower brain temperature. Brain temperature could conceivably be lowered more rapidly by cooling only the head. The common carotid artery runs lateral to the pharynx, about 1 cm away. When the pharynx is cooled, the common carotid artery is cooled and brain temperature is reduced hematogenously. The present study verifies the brain hypothermia effect of pharyngeal cooling performed during resuscitation after cardiac arrest, and investigates whether this approach improves neurological prognosis and life prognosis.

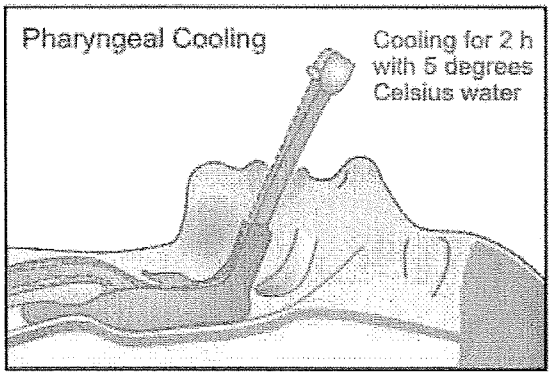

After securing the airway by tracheal intubation, a pharyngeal cooling cuff is inserted. The pharyngeal cooling cuff is constructed to fit the shape of the pharynx. Physiological saline (5 degrees Celsius) is perfused into the cuff at 500 mL/min.

【英文ページ、咽頭冷却カフの説明】

Health and Labour Sciences Research Grant (Translational Research)

Investigation of Clinical Utility of Pharyngeal Cooling During Resuscitation

Multicenter Clinical Study 〈I-Cool〉

Top Page
Organization
What is Pharyngeal Cooling?
Pharyngeal Cooling Cuff
Circulator
Protocol
日本語ページ

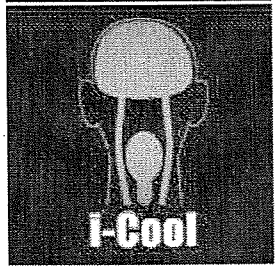

Pharyngeal Cooling Cuff

The cuff is made of vinyl chloride and has passed biological safety tests. The cuff was developed based on 3D-CT models of the pharynx, and can be easily inserted into the pharynx using the same technique used with an esophageal obturator airway. As the carotid artery runs posterolateral to the pharynx, adhesion to the posterolateral mucosa is increased. The inside of the cuff (balloon, pressure limit: 200 cmH2O) is perfused with physiological saline at a rate of 500 mL/min and a pressure of 50 cm H2O.

Development of Pharyngeal Cooling Cuff

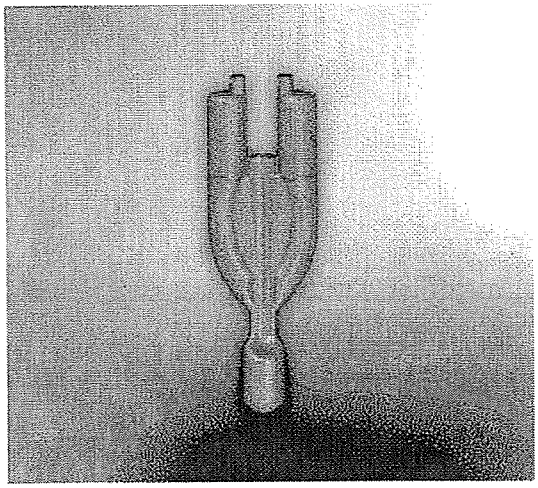

Cuff was developed based on CAD

【英文ページ、潅流装置の説明】

Health and Labour Sciences Research Grant (Translational Research)

Investigation of Clinical Utility of Pharyngeal Cooling During Resuscitation

Multicenter Clinical Study 〈i-Cool〉

Top Page
Organization
What is Pharyngeal Cooling?
Pharyngeal Cooling Cuff
Circulator
Protocol
日本語ページ

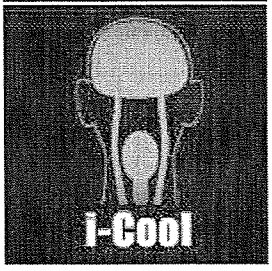

Circulator

The circulator has the capability to rapidly cool physiological saline and perfuse it into the pharyngeal cooling cuff at a rate of 500 mL/min. Sensors built into the pharyngeal cooling cuff collect internal pressure and temperature data every 4 ms, controlling these variables in real time.

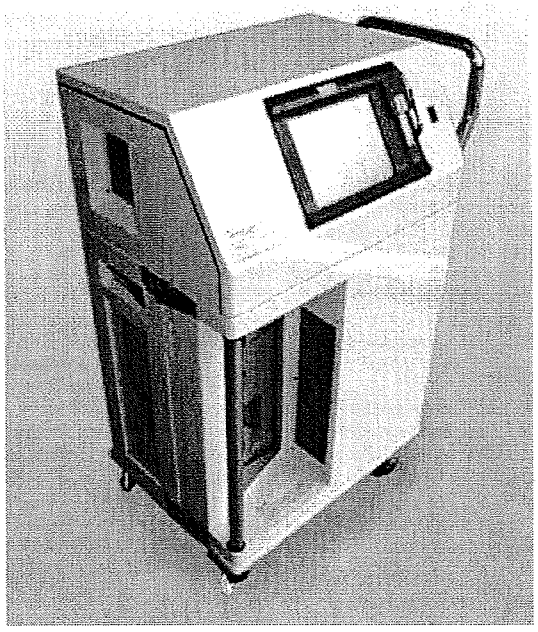

Tympanic thermometer

Tympanic thermometer

Neuroscience Letters 449 (2009) 61–65

Contents lists available at ScienceDirect

Neuroscience Letters

journal homepage: www.elsevier.com/locate/neulet

Dynamic changes in cortical NADH fluorescence in rat focal ischemia: Evaluation of the effects of hypothermia on propagation of peri-infarct depolarization by temporal and spatial analysis

Toshihiro Sasaki*, Yoshimasa Takeda, Hideki Taninishi, Minako Arai, Kensuke Shiraishi, Kiyoshi Morita

Department of Anesthesiology and Resuscitology, Okayama University Medical School, 2-5-1 Shikata-cho, Okayama City, Okayama 700-8558, Japan

ARTICLE INFO

Article history:
Received 8 August 2008
Received in revised form 8 October 2008
Accepted 14 October 2008

Keywords:
Focal cerebral ischemia
Hypothermia
Peri-infarct depolarization
DC potential
NADH
NADH fluorescence

ABSTRACT

Suppression of peri-infarct depolarizations (PIDs) is one of the major mechanisms of hypothermic protection against transient focal cerebral ischemia. Previous studies have shown the lack of hypothermic protection against permanent focal ischemia. We hypothesized the lack of hypothermic protection was due to the poor efficacy in suppression of PIDs. To examine the hypothesis, we elucidated the effects of hypothermia on the manner of propagation of PIDs with temporal and spatial resolutions using NADH (reduced nicotinamide adenine dinucleotide) fluorescence images by illuminating the parietal–temporal cortex with ultraviolet light. Spontaneously hypertensive rats ($n = 14$) were subjected to permanent focal ischemia by occlusion of the middle cerebral and left common carotid arteries. 2-h hypothermia (30 °C) was initiated before ischemia. Although hypothermia delayed the appearance of PIDs, it did not suppress their appearance. Furthermore, 54% of the PIDs enlarged the high-intensity area of NADH fluorescence in the hypothermia group, similar to the normothermia group (53%). The high-intensity area of NADH fluorescence widened by each PID was larger in the hypothermia group than in the normothermia group. These findings suggest that PIDs even in hypothermia are one of the major factors causing growth of infarction, emphasizing the importance of therapy that targets suppression of PIDs even during hypothermia.

Peri-infarct depolarizations (PIDs) are thought to contribute to infarct expansion because of a positive relationship between infarct volume and number of PIDs [9,12,13]. A previous study using a transient focal cerebral ischemia model showed by using focal detection of PIDs (i.e., glass microelectrodes) that hypothermia decreased the frequency of PIDs [4]. This finding suggested that the protective effect of hypothermia in transient focal ischemia is mediated through suppression of PIDs. On the other hand, other studies have shown that hypothermia has no protective effect in permanent focal ischemia [14,15]. However, little is known about the reason for the lack of hypothermic protection in permanent focal ischemia. We hypothesized that the lack of hypothermic protection against permanent focal ischemia was due to the poor effect of hypothermia on suppression of PIDs.

We have reported an NADH fluorescence imaging method for detection of PIDs that allows a more global measurement of PIDs [8]. In the present study, we used this method to examine the above-stated hypothesis and elucidated the effects of hypothermia on the manner of propagation of PIDs in rats with permanent focal cerebral ischemia.

This study was approved by the Animal Research Control Committee of Okayama University Medical School. Male spontaneously hypertensive rats (SHRs) (Charles River Japan, Yokohama, Japan), weighing 320 ± 40 g, were anesthetized with 5% halothane in oxygen after an overnight fast. After endotracheal intubation, anesthesia was maintained by artificial ventilation with 1% halothane mixed with 70% nitrous oxide in 30% oxygen. The right femoral artery was cannulated for blood pressure monitoring and blood sampling. Arterial blood gases were measured before and during ischemia and maintained within the normal range. The mean arterial pressure was above 60 mmHg throughout the experiment. After placement in a stereotaxic apparatus (Narishige, Tokyo, Japan), a large cranial window (9 mm × 11 mm) was prepared on the left parietal–temporal bone for the measurement of images of NADH fluorescence. The dura was kept intact. To analyze the correlation between changes in NADH fluorescence, direct current (DC) deflection and cerebral blood flow (CBF), two DC electrodes (tip diameter <5 μm) were placed in the anterior and posterior cortexes (depth of 750 μm, 0–2 mm anterior and 2–3 mm lateral to the bregma, 2–4 mm posterior and 2–4 mm lateral to the bregma, respectively)

* Corresponding author. Tel.: +81 86 235 7327; fax: +81 86 235 7329.
E-mail address: tooshy@md.okayama-u.ac.jp (T. Sasaki).

0304-3940/$ – see front matter © 2008 Elsevier Ireland Ltd. All rights reserved.
doi:10.1016/j.neulet.2008.10.054

and a laser-Doppler flow probe (ALF2100, Advance, Tokyo) was placed adjacent to one of the two DC electrodes.

The animals were randomly assigned to two groups: a normothermia group ($n=7$) and a hypothermia group ($n=7$). In the normothermia group, rectal temperature was maintained throughout the experiment at 37.0±0.5 °C using a heated water blanket. In the hypothermia group, rectal temperature was maintained before ischemia at 30.0±0.5 °C using a water blanket and ice packs. Brain surface temperature was controlled with a gentle flow of warm saline (37 °C in the normothermia group and 30 °C in the hypothermia group) perfused over the skull surface, because brain temperature was 1.0±0.5 °C below the drip temperature, as determined in a pilot study.

NADH fluorescence imaging was started and permanent focal cerebral ischemia was initiated by ligating the left common carotid artery and by lifting the middle cerebral artery (MCA) 1 mm above the cortical surface and cauterizing it. Brint et al. [3] reported that the infarct volume is highly reproducible in SHR compared with Wistar and Fisher rats.

The technique used for cortical NADH fluorescence imaging was described in detail previously [7,8]. In brief, the cortical surface was illuminated with UV light (366-nm). Images of NADH fluorescence were obtained by using a CCD camera (ST-6UV; SBIG, Santa Barbara, CA) with a 460-nm bandpass filter. Images (170 × 170 pixels, width × height) were taken every 15 s. Data for each pixel in each image of NADH fluorescence were divided by those of the control image obtained before the initiation of focal ischemia, and the percent change in NADH fluorescence was expressed in each pixel with 256 gray scales. Two hours after the onset of ischemia, imaging was stopped and the hypothermic animals were rewarmed to 36.5 °C over a period of 60 min. The wounds were closed and the rats were extubated and returned to their cages with free access to food and

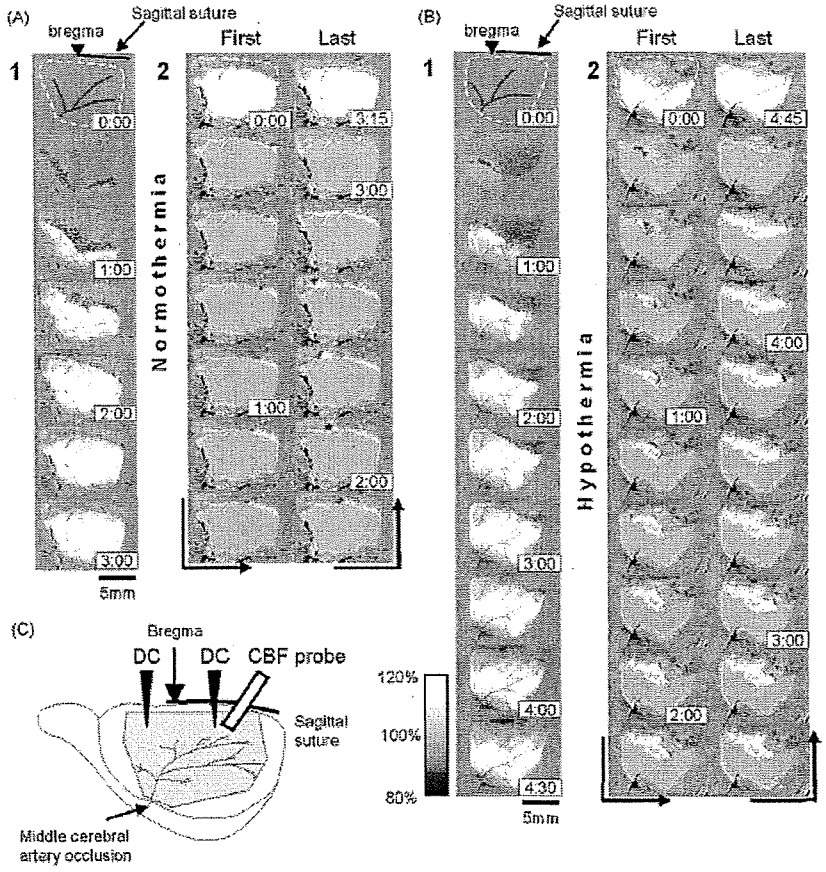

Fig. 1. (A and B) Sequences of NADH fluorescence images. (C) A schematic drawing of the cranial window. The dashed lines in (A) and (B) represent the cranial window. For visualization of changes in NADH fluorescence, data for each pixel in each image of NADH fluorescence were divided by those of the control image obtained before the initiation of focal ischemia, and the percent change in NADH fluorescence was expressed in each pixel with 256 gray scales. A wave front (red), detected by subtracting the neighboring image, is superimposed on each image. (A1 and B1) Formation of high-intensity area of NADH fluorescence following the initiation of ischemia under normothermia (A) and hypothermia (B). The first image was taken before ischemia. Images were taken every 30 s. The high-intensity area of NADH fluorescence spread from the area of middle cerebral artery occlusion and formed rapidly after the initiation of ischemia. (A2 and B2) Sequence images; the first and last images are arranged at the top. The high-intensity area shows more than 120% NADH fluorescence (green) in the first images and is superimposed on each image. Images were taken every 15 s. (A2) The first image was taken 32 min after the onset of ischemia. A high-intensity wave of fluorescence, originating from the posterior region, propagated along the high-intensity area of NADH fluorescence in an anterior direction. (B2) The first image was taken 42 min after the onset of ischemia. A high-intensity wave of fluorescence, originating from the parietal cortex, propagated along the ischemic core in anterior and posterior directions. As shown in the last image, the area showing more than 120% NADH fluorescence (blue) remained in the region surrounding the high-intensity area of NADH fluorescence after the passage of the high intensity wave of fluorescence.

water. Four rats underwent a sham operation in which the hook was placed in contact with a portion of the MCA and removed without lifting the artery.

Twenty-four hours after the onset of ischemia, all animals were anesthetized with 3% halothane. After inserting a cannula into the ascending aorta, each animal was perfused with heparinized physiologic saline (20 units/mL) and 6% paraformaldehyde in 0.1 mol/mL phosphate buffer (pH 7.4). To identify the area of the cranial window, the margin of the area was marked by using a 27-gauge needle with blue ink before enucleating the brain. After brain removal and paraffin-embedding, brain sections (5-μm thick) were prepared at 250-μm intervals, stained with hematoxylin and eosin, examined and photographed. The images were analyzed for the infarct areas by a researcher blinded to the test procedure. Right hemispheric and infarct volumes were calculated by multiplying infarct areas by slice thickness and integration over all slices. Infarct volumes are expressed as percentage of right hemispheric volume.

Linear regression models were used to evaluate the correlation between percent changes in NADH fluorescence and magnitude of negative DC deflection. Values are expressed as means ± S.D. Parameters obtained by analysis of NADH fluorescence images and infarct volumes were compared between the normothermia and hypothermia groups using Student's *t*-test. A *p*-value <0.05 was considered significant in all statistical tests.

Fig. 1 shows serial changes in NADH fluorescence under ischemia with hypothermia or normothermia. The initiation of ischemia was immediately followed by 5% increase in intensity of NADH fluorescence in the vicinity of the proximal region of the MCA due to a rapid decrease in CBF. A high-intensity area of NADH fluorescence formed from the proximal to distal region of the MCA in 185 ± 25 and 354 ± 105 s in the normothermia group and hypothermia group, respectively (A1 and B1). Several minutes after the formation of the high-intensity area, high-intensity waves of fluorescence were observed at the edge of the high-intensity area, which propagated around the area to a width of 1.5–3 mm. Because the high-intensity area of fluorescence formed nearer to the proximal region of the MCA in the hypothermia group, the high-intensity waves of fluorescence propagated nearer to the proximal region of the MCA in the hypothermia group (A2 and B2). Seventeen waves and 13 waves were observed in the normothermia group and hypothermia group, respectively during the observation period. Nine of the 17 waves in the normothermia group and 7 of the 13 waves in the hypothermia group did not disappear and eventually enlarged the high-intensity area of NADH fluorescence, while the others disappeared without leaving any traces.

The DC potential was successfully measured at 12 sites in the normothermia group and at 12 sites in the hypothermia group. Ten of the 30 high-intensity waves of fluorescence moved over the DC recording sites. As shown in Fig. 2, the DC recording was divided into four types. Table 1 summarizes the number of DC deflection types at each recording site. Because the waveform of fluorescence

Table 1
Number of DC deflection types in each recording site.

	Type 1	Type 2	Type 3	Type 4
Anterior region				
Normothermia (*n* = 6)	0	4	1	1
Hypothermia (*n* = 5)	2	3	0	0
Posterior region				
Normothermia (*n* = 6)	1	0	0	5
Hypothermia (*n* = 7)	4	2	0	1
Total				
Normothermia (*n* = 12)	1	4	1	6
Hypothermia (*n* = 12)	6	5	0	1

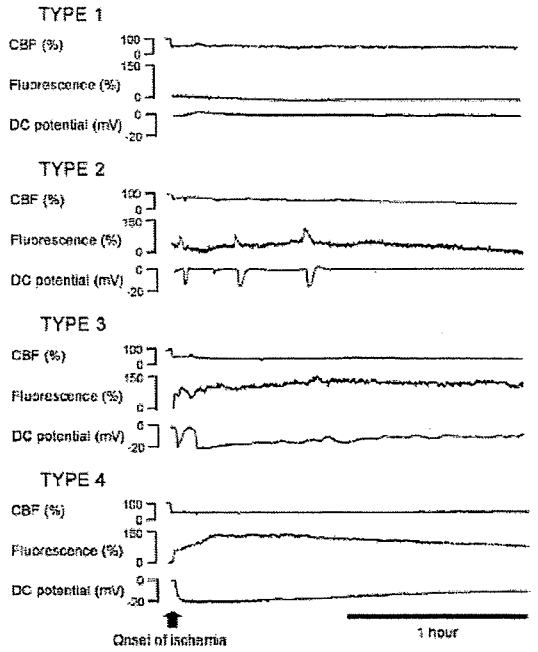

Fig. 2. Direct current (DC) recordings were classified into four types: type 1, in which no DC deflection was observed; type 2, in which DC potential showed recurrent depolarization; type 3, in which DC potential showed recurrent depolarization and eventually persistent depolarization; and type 4, in which persistent depolarization was observed. The waveform of NADH fluorescence was analogous to that of the DC potential. Cerebral blood flow was stable and not affected by depolarizations.

was analogous to that of the DC potential, the high-intensity waves of fluorescence were defined as PIDs in this study, as described previously [8,16,17]. CBF was almost stable for 2 h after the onset of ischemia and was not generally affected by the propagation of waves. In sham-operated SHR, no changes in DC potential or fluorescence were observed for 2 h after the onset of ischemia. The peak value of fluorescence (percent change from the control) of waves was closely related to the magnitude of negative DC deflection ($r = 0.623$, $p = 0.01$ in the normothermia group; $r = 0.663$, $p = 0.02$ in the hypothermia group). Due to the similarities in the linear regression relationships between the normothermia and hypothermia groups and the fact that 20 mV magnitude of negative DC deflection corresponded to 120% of the control level of NADH fluorescence (Fig. 3), we measured the area persistently showing more than 120% NADH fluorescence in this study.

As shown in Fig. 4, the area with persistently high fluorescence (>120% NADH) increased gradually, reached a peak level and then plateaued. Although the area was larger in the normothermia group relative to that in the normothermia group during the observation period, the difference between the areas in the two groups became smaller with time. PIDs were observed from 5 to 47 min after the onset of ischemia in the normothermia group and from 15 to 76 min after the onset of ischemia in the hypothermia group. No more PIDs were observed in either group thereafter during the observation period.

Table 2 summarizes the characteristics of PIDs. The frequencies of PIDs per rat were not significantly different between the two temperature groups ($p = 0.2$). The appearance of the first and second PIDs was delayed in the hypothermia group compared

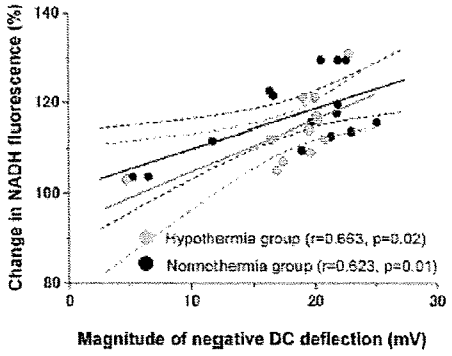

Fig. 3. Relationship between % changes in NADH fluorescence and magnitude of negative DC deflection. Note the overlap of 95% confidence intervals of the two groups.

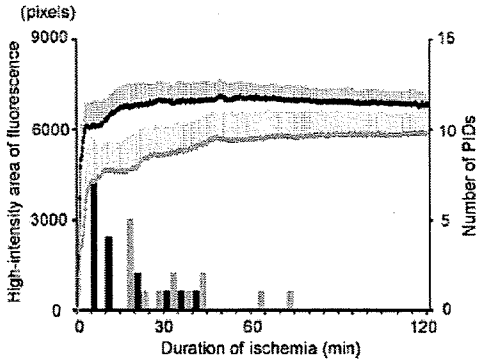

Fig. 4. Change in the high-intensity area of fluorescence and frequency distribution of peri-infarct depolarizations (PIDs). The line graph shows the high-intensity area corresponding to the number of pixels showing more than 120% NADH fluorescence. Black line: normothermia group, gray line: hypothermia group. The bar graph shows the frequency distribution of PIDs in the normothermia group (black) and hypothermia group (gray). Data were pooled in 5-min intervals.

with the normothermia group ($p < 0.001$ and $p = 0.01$, respectively). The rate of propagation of PIDs was significantly slower in the hypothermia group than in the normothermia group ($p < 0.001$). The high-intensity area enlarged by each PID was significantly larger in the hypothermia group than in the normothermia group ($p = 0.009$). The location of the margin of the enlarged area was identified on the stained brain sections by measuring the distance from the edge of the cranial window. The enlarged area was located within infarct area.

Table 2
Characteristics of peri-infarct depolarizations (PIDs).

	Normothermia ($n=7$)	Hypothermia ($n=7$)
Frequency of PIDs (times/rat)	2.4 ± 0.5	1.9 ± 1.1
Propagation rate (mm/min)	2.8 ± 0.5	1.7 ± 0.2*
Area enlarged by each PID (pixels)	470 ± 210	980 ± 449*
Time of the first PID appearance (min)	8.1 ± 1.8	19.9 ± 4.1**
Time of the second PID appearance (min)	21.0 ± 12.8	40.8 ± 5.4**

Data are mean ± S.D.
* $p < 0.01$, compared with the normothermia group (by Student's t-test).
** $p < 0.05$.

The percent infarct volume 24 h after the onset of ischemia in the hypothermia group (24.3 ± 3.9%) was significantly smaller than that in the normothermia group (32.9 ± 4.5%, $p = 0.003$).

The signal intensity of NADH fluorescence *in vivo* can be affected by numerous factors other than changes in NADH content (e.g., changes in hemoglobin concentration, scattering of light, ratio of oxyhemoglobin to deoxyhemoglobin, and ratio of protein-binding NADH to free NADH). Although we expected that changes in CBF would greatly alter the signal intensity of NADH fluorescence, there was only 5% change in NADH fluorescence in the vicinity of the MCA caused by a rapid decrease in CBF immediately after the onset of ischemia and CBF was almost stable thereafter. Previous studies showed that PIDs are not accompanied by significant increases in CBF as in normal spreading depressions [1,9,11] because the capacity of collateral perfusion is reduced in such regions showing severe CBF reduction [5] and that NADH content increased to up to 230% of the control level during passage of depolarization [7]. Therefore, the increase in NADH fluorescence during passage of PIDs and the increase in the high-intensity area of NADH fluorescence by PIDs are due to changes in NADH content rather than changes in CBF.

In the present study, we found PID generation even in hypothermic rats and no significant difference between the frequency of PIDs per rat in the normothermia group and that in the hypothermia group. This result is inconsistent with the results of a previous study reported by Chen et al. [4], who showed lack of PID generation in hypothermic rats. Possible reasons for this inconsistency include differences in the focal ischemia model used in the two studies. Chen et al. [4] used Wistar rats and focal ischemia was induced by the intraluminal filament method. On the other hand, we used SHR and focal ischemia was induced by occluding the left middle cerebral and left common carotid arteries. In this regard, a previous study [15] showed that hypothermia induced by the same method was more protective in Wistar rats than in SHR. While CBF is gradually decreased by the intraluminal filament method [6], CBF is steeply reduced by our method. These systematic differences among rat strains and methodological variations of vascular occlusion may contribute to the inconsistency. Another possible reason for the inconsistency is the difference in the methods used for measurement of PIDs. While Chen et al. [4] measured PIDs at two specific points by using DC electrodes, we used the two-dimensional technique of NADH fluorescence imaging that allows observation of almost the entire left hemisphere. The NADH fluorescence images highlighted the presence of differences in areas of propagation of PIDs under normothermia and hypothermia. The area of propagation of PIDs in hypothermic animals shifted to the proximal region of the MCA. Since the minimum width of PIDs was 1.5 mm in hypothermic animals, propagation of PIDs in the hypothermic rats could be missed if the frequency of PIDs is measured by DC electrodes.

Although we did not find a reduction of PID frequency during hypothermia, the 2-h hypothermia (30 °C) induced before permanent occlusion of the MCA was protective. As shown in Fig. 4, reduction of the high-intensity area of fluorescence soon after the onset of ischemia in the hypothermic rats was sustained for 2 h after the onset of ischemia, although the difference between the areas in two groups became smaller with elapse of time. Therefore, we speculate that reduction of the high-intensity area contributed to the decrease in infarct volume. The high-intensity area rapidly widened in the first 15 min after the onset of ischemia in the normothermic rats. This result suggests that hypothermia should be initiated within 15 min after the onset of ischemia. Consistent with this suggestion, a previous study reported that 2-h hypothermia (30 °C) induced 15 min after ischemia was not protective in the same model of focal ischemia [15].

In the present study, 54% of the PIDs in the hypothermic rats enlarged the high-intensity area of fluorescence, similar to that seen in normothermia (53%). In addition, we found that the area enlarged by each PID was significantly larger in hypothermia than in normothermia. Since the increase in NADH fluorescence indicates disproportion in oxygen balance [11] and correlates with low ATP and high lactate levels [18], and since the cortex corresponding to the enlarged area showed infarction 24 h after the onset of ischemia in the present study, we suggest that PIDs in hypothermia contribute to the increase in infarct volume more than those in normothermia and that therapies designed to prevent the development of PIDs in the presence of hypothermia might be important in any treatment strategy designed for stroke. This conclusion is supported by the results of a study by Ikonomidou et al. [10] demonstrating that hypothermia combined with MK-801, an NMDA antagonist, is more effective against hypoxic/ischemic brain damage than hypothermia or MK-801 alone.

NADH fluorescence images showed that hypothermia delayed the initiation of the first and second PIDs. Since PIDs can be suppressed by administration of glutamate antagonists [9,13] and since PIDs are initiated at the edge of the ischemic core, the increase in glutamate in the margin of the ischemic core is considered to be related to the mechanism of initiation of PIDs. Baker et al. [2] found that hypothermia delayed the increase in glutamate tissue concentration in the ischemic core. Thus, it is possible that the delay in increase in glutamate in the ischemic core during hypothermia is due to a delay in the initiation of PIDs.

In conclusion, we elucidated the effects of hypothermia on the manner of propagation of PIDs with temporal and spatial resolutions by using NADH fluorescence images. Although hypothermia delayed the appearance of PIDs, it did not suppress the occurrence of PIDs. Therefore, we suggest that the lack of hypothermic protection against permanent focal ischemia contributed to the lack of reduction in PID generation. The high-intensity area of NADH fluorescence that was enlarged by each PID was larger in hypothermia than in normothermia. These results suggest that PIDs in hypothermia could have a greater effect on growth of infarction than those in normothermia. These findings emphasize the importance of therapies designed to suppress PIDs even during hypothermia in the acute stage of focal ischemia.

Acknowledgement

This study was supported by a grant from the Ministry of Education, Culture, Sports, and Technology of Japan (20591804).

Appendix A. Supplementary data

Supplementary data associated with this article can be found, in the online version, at doi:10.1016/j.neulet.2008.10.054.

References

[1] T. Back, K. Kohno, K.A. Hossmann, Cortical negative DC deflection following middle cerebral artery occlusion and KCl-induced spreading depression: effect on blood flow, tissue oxygenation, and electroencephalogram, J. Cerebral Blood Flow Metab. 14 (1994) 12–19.
[2] C.J. Baker, A.J. Fiore, V.J. Frazzini, T.F. Choudhri, G.P. Zubay, R.A. Solomon, Intraischemic hypothermia decrease the release of glutamate in the cores of permanent focal cerebral infarcts, Neurosurgery 36 (1995) 994–1001.
[3] S. Brint, M. Jacewicz, M. Kiessling, J. Tanabe, W. Pulsinelli, Focal brain ischemia in the rat: methods for reproducible neocortical infarction using tandem occlusion of the distal middle cerebral and ipsilateral common carotid arteries, J. Cerebral Blood Flow Metab. 8 (1988) 474–485.
[4] Q. Chen, M. Chopp, G. Bodzin, H. Chen, Temperature modulation of cerebral depolarization during focal cerebral ischemia in rats: correlation with ischemic injury, J. Cerebral Blood Flow Metab. 13 (1993) 389–394.
[5] H. Date, K.A. Hossmann, T. Shima, Effect of middle cerebral artery compression on pial artery pressure, blood flow, and electrophysiological function of cerebral cortex of cat, J. Cerebral Blood Flow Metab. 4 (1984) 593–598.
[6] H. Harada, Y. Wang, Y. Mishima, N. Uehara, T. Makaya, T. Kano, A novel method of detecting rCBF with laser-Doppler flowmetry without cranial window through the skull for a MCAO rat model, Brain Res. 14 (2005) 165–170.
[7] M. Hashimoto, Y. Takeda, T. Sato, H. Kawahara, O. Nagano, M. Hirakawa, Dynamic changes of NADH fluorescence images and NADH content during spreading depression in the cerebral cortex of gerbils, Brain Res. 872 (2000) 294–300.
[8] T. Higuchi, Y. Takeda, M. Hashimoto, O. Nagano, H. Hirakawa, Dynamic changes in cortical NADH fluorescence and direct current potential in rat focal ischemia: relationship between propagation of recurrent depolarization and growth of the ischemic core, J. Cerebral Blood Flow Metab. 22 (2002) 71–79.
[9] T. Iijima, G. Mies, K.-A. Hossmann, Repeated negative DC deflections in rat cortex following middle cerebral artery occlusion are abolished by MK-801: effect on volume of ischemic injury, J. Cerebral Blood Flow Metab. 12 (1992) 727–733.
[10] C. Ikonomidou, J.L. Mosinger, J.W. Olney, Hypothermia enhances protective effect of MK-801 against hypoxic/ischemic brain damage in infant rats, Brain Res. 487 (1989) 184–187.
[11] A. Mayevsky, N. Zarchin, C.M. Friedli, Factors affecting the oxygen balance in the awake cerebral cortex exposed to spreading depression, Brain Res. 236 (1982) 93–105.
[12] G. Mies, T. Iijima, K.A. Hossmann, Correlation between periinfarct DC shifts and ischemic neuronal damage in rat, Neuroreport 4 (1993) 709–711.
[13] G. Mies, K. Kohno, K.A. Hossmann, Prevention of periinfarct direct current shifts with glutamate antagonist NBQX following occlusion of the middle cerebral artery in the rat, J. Cerebral Blood Flow Metab. 14 (1994) 802–807.
[14] T.R. Ridenour, D.S. Warner, M.M. Todd, A.C. McAllister, Mild hypothermia reduces infarct size resulting from temporary but not permanent focal ischemia in rats, Stroke 23 (1992) 733–738.
[15] Y. Ren, M. Hashimoto, W.A. Pulsinelli, T.S. Nowak Jr., Hypothermic protection in rat focal ischemia models: strain differences and relevance to "reperfusion injury", J. Cerebral Blood Flow Metab. 24 (2003) 42–53.
[16] A.J. Strong, S.P. Harland, B.S. Meldrum, D.J. Whittington, The use of in vivo fluorescence image sequences to indicate the occurrence and propagation of transient focal depolarizations in cerebral ischemia, J. Cerebral Blood Flow Metab. 16 (1996) 367–377.
[17] A.J. Strong, S.E. Smith, D.J. Whittington, B.S. Meldrum, A. Parsons, J. Krupinski, A.J. Hunter, S. Patel, C. Robertson, Factors influencing the frequency of fluorescence transients as markers of peri-infarct depolarizations in focal cerebral ischemia, Stroke 31 (2000) 214–222.
[18] F.A. Welsh, V.R. Marcy, R.E. Sims, NADH fluorescence and regional energy metabolites during focal ischemic and reperfusion of rat brain, J. Cerebral Blood Flow Metab. 11 (1991) 459–465.

Journal of Biomechanical Science and Engineering

Vol. 5, No. 1, 2010

Heat Transfer Characteristics of a Pharyngeal Cooling Cuff for the Treatment of Brain Hypothermia*

Koji FUMOTO**, Yoshimasa TAKEDA***, Hiroshi HASHIMOTO****, Masatomo KOKUBU**** and Tsuyoshi KAWANAMI*****

**Department of Mechanical Engineering, Kushiro National College of Technology, Otanoshike-Nishi 2-32-1, Kushiro, Hokkaido 084-0916, Japan
E-mail: fumoto@mech.kushiro-ct.ac.jp

***Department of Anesthesiology and Resuscitology, Graduate School of Medicine, Dentistry, and Pharmaceutical Sciences, Okayama University, 2-5-1, Shikada-cho, Okayama 700-8558, Japan

****Daiken Medical Co., Ltd., 2-6-2, Ayumino, Izumi, Osaka 594-1157, Japan

*****Division of Mechanical Engineering, Graduate School of Engineering, Kobe University, 1-1, Rokkodai-cho, Nada-ku, Kobe, Hyougo 657-8501, Japan

Abstract

In the present study, the characteristics of both flow and heat transfer in a pharyngeal cooling cuff for the treatment of brain hypothermia were investigated experimentally and numerically. The pharyngeal cooling cuff, which is a balloon-like structure placed in the pharynx, was developed for medical purposes. As a method for controlling the brain temperature, cooling water, which is physiological saline at 5°C, is injected into the cuff in order to cool the common carotid artery, which is adjacent to the pharynx. In this study, the heat transfer characteristics between the cuff wall and phantom body, which was considered to be equivalent to the human body, were experimentally determined, and the flow behaviour in the cuff was observed in detail. Furthermore, a three-dimensional numerical simulation was carried out to investigate both the flow velocity and temperature distribution in the cuff.

Key words: Pharyngeal Cooling, Brain Hypothermia, Medical Engineering, Numerical Simulation, Heat Transfer

1. Introduction

In Japan, cerebropathy, including cerebrovascular disorder, is one of the causes of death following malignant neoplasms and heart diseases[1]. Crisis prediction in the case of cerebrovascular disorders and elucidation of the mechanism underlying the development of these disorders are the need of the day. Further, the establishment of a good method for treating the recurrence of neurological condition, including the society return, is strongly desired. Hayashi[2]~[3] revealed that one of the therapies for lowering the brain temperature in the case of serious wound injuries to the head, severe cerebrovascular disorders, or brain ischemia was cardiopulmonary stop; Patients treated with this method were found to have a good neurological prognosis[4]~[5]. At present, low-temperature brain therapy enables the controls of the brain temperature and intracranial pressure in the case of patients with severe brain damage who satisfy the condition variously. This therapy has been introduced to repair nerve cells damaged during the initial brain damage, and to prevent the development of secondary brain damage. Since the release of neurotransmitters and action of free radicals are both drastically suppressed at brain temperatures of 32°C or less, it is said that

*Received 8 June, 2009 (No. 09-0252)
[DOI: 10.1299/jbse.5.85]

the brain is protected against damage. For the purpose of treatment, brain hypothermia is divided into mild hypothermia (core temperature, 34°C) and moderate hypothermia (32°C). The temperature of the brain is lowered and maintained at low temperatures by lowering the body temperature. The latter is achieved by covering the whole body with a water-cooled blanket. In this method, the patient's body is wrapped with a water-cooled blanket, and cold water (approximately 20°C) is circulated through the blanket. It is also possible to simultaneously maintain the brain temperature at the desired degree and strictly monitor the temperature. However, this management strategy, i.e., conventional hypothermia treatment, requires a great deal of time to bring about changes in body temperature and for acute state transition of the pathology. Therefore, research and development on medical instruments such as water-cooling blankets, headgear, and mufflers for the purpose of cooling of body parts and lowering the brain temperature are widely being conducted[6].

Takeda et al.[7]~[8] developed the pharyngeal cooling cuff by analyzing the anatomy of the pharynx division. This cuff is inserted through the oral cavity of the patient, and it can cool the common carotid artery, which is located approximately 10 mm outside the pharynx division. Thus, cooling and temperature control of the brain is possible via the cooling of the main blood vessel that supplies the brain. In comparison with conventional whole-body cooling, the pharyngeal cuff method rapidly lowers the brain temperature. Moreover, the countermeasures of acute brain temperature management and early brain cooling during life-threatening emergencies related to brain diseases are possible with the latter method. For acute phase of brain cooling, we assume that physiological saline at 5°C should be used to cool the cuff. During animal testing[9], this cuff has been shown to produce a good cooling effect on the brain. However, the optimum cooling efficiency of this cuff has not been determined since the structure of this device is based on the pharynx shape.

On the basis of this background, we aimed to understand the flow and heat transfer characteristics of the pharyngeal cooling cuff. In this report, in order to evaluate pharyngeal cooling, we analyzed the heat transfer between the cuff and a phantom body (hereafter referred to as phantom), which was considered to be equivalent to the human body. In particular, we focused on the thermal transport characteristics within the cuff. Further, computational fluid dynamics (CFD) analysis was carried out to analyze the flow in the cuff, and the cooling efficiency was examined under various conditions. These results are useful as they provide the basic information required to develop the clinical applications of the cuff and to improve the cuff to ensure better cooling of the pharynx. Future studies will address transport within the surrounding tissue and the effectiveness of carotid artery blood cooling.

Nomenclature

D	:	Diameter
L	:	Length
Q	:	Heat quantity
q	:	Heat flux
S	:	Surface area
T	:	Temperature
ΔT	:	Temperature difference t
U	:	Velocity
V	:	Inlet flow
X	:	Local position
η	:	Cooling efficiency
ρ	:	Density

Subscript

1~6	:	Thermocouple
in	:	Inflow
L	:	Liquid phase
out	:	Outflow
Pha	:	Phantom

2. Experimental setup and procedures

2.1. Pharyngeal cooling cuff

The structure of the pharyngeal cooling cuff and a schematic diagram of the working of the cooling cuff are shown in Figures 1 and 2, respectively. In the case of patients with difficulties in voluntary respiration, the pharyngeal cooling cuff is inserted into the pharynx division along with the tube for artificial respiration. Therefore, the shape of the cuff is based on the shape of the pharynx division. The upper and lower parts of the cuff are placed in the pharynx and upper esophageal divisions, respectively. The cooling cuff, which is a balloon-like structure, is 0.5 mm in thickness and made of polyvinyl. It is 250 mm long with a total volume of 100 ml. The cooling cuff has an inlet tube and 2 outlet tubes, which are 4 mm in diameter. The basic flow behavior within the cooling cuff is as follows. Cooling water, which is physiological saline at around 5°C, flows into the inlet tube. The cooling water passes through the cuff and reaches the tip of the cuff. At the tip, the inlet

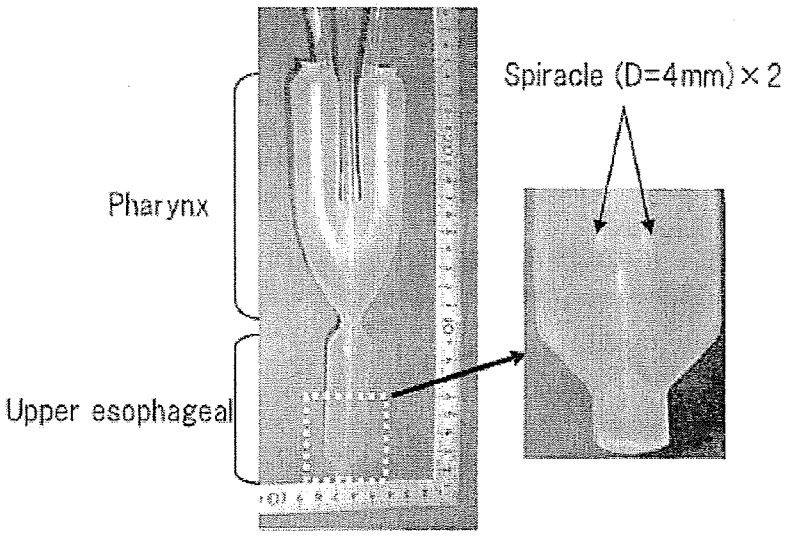

Figure 1 Appearance of pharyngeal cooling cuff

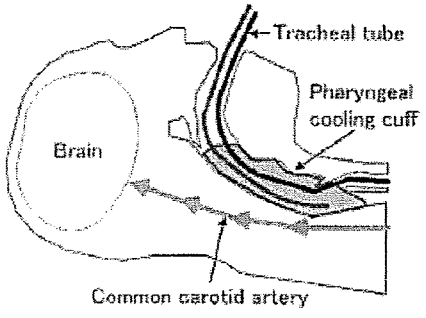

Figure 2 Image of the pharyngeal cooling cuff for brain hypothermia treatment